



AN INVESTIGATION OF
TIP VORTICES IN A WATER TUNNEL

D.H. FRUMAN*

ABSTRACT

This paper deals with the problem of a tip vortex issuing from a finite span hydrofoil. The investigation was conducted in a water instead of a wind tunnel to benefit from the larger Reynolds numbers achieved using smaller test models as well as the possibility to use cavitation within the vortex core as a tracer to investigate its stability and diffusion. In this work the tangential and axial velocities in a tip vortex generated by a finite span hydrofoil of elliptical planform and symmetrical cross section have been measured using LDA at a distance of several chords downstream. The tangential velocity profiles obtained for various operating conditions clearly show the existence of a core region rotating as a rigid body and a nearly potential region outside. Estimates of the circulation in this region were obtained by fitting the Burgers model to the velocity data. Fair agreement between the circulation deduced from the velocity profile and lift measurements was obtained. Some visualisations of the cavitation induced by the tip vortex on a two dimensional hydrofoil at several chord lengths downstream are also presented. It is shown that the velocities induced by the vortex cause a modification of the effective angle of attack along the leading edge of the two dimensional hydrofoil and give rise to a distinct separation region on its surface. The latter problem is important in connection with the operation of helicopter rotor blades.

* Professor and Research Group Leader, Groupe Phénomènes d'Interface, Ecole Nationale Supérieure de Techniques Avancées, 91120 Palaiseau, FRANCE.

I- INTRODUCTION

Tip vortices and tip vortex-wing interaction have been the subject of a significant amount of research efforts stemming from the effects associated with these phenomena. For example, in aerodynamics, small planes can be overturned when passing through the tip vortices of large planes and the velocities induced by the rotating flow can alter the flow on appendages situated downstream of the generating airfoil. In hydrodynamics, cavitation may occur in the low pressure region of the vortices and be the source of radiated noise and other nuisances such as cavitation induced on stern rudders behind screw propellers. Most of the investigations have been aimed at the modelling of the tangential velocity distributions and its decay by diffusion [1], at the design of effective ways to increase such a diffusion by modifying the initial roll-up conditions [2] or the fluid rheological properties [3], at the vortex-wing interaction [4], at the cavitation inception and radiated noise [5], etc..

In the course of our investigation of tip vortex cavitation inhibition by polymer additive ejection from the tip of the generating hydrofoil [3] a certain amount of data relevant to aerodynamics has been obtained. In particular, the tangential and axial velocity distributions in non cavitating conditions have been measured for a variety of flow situations. These measurements extend those of BAKER *et al* [1] and other authors. Moreover, since cavitation can be used as a natural tracer of the core of the vortex as well as of the flow modifications induced over downstream structures, qualitative information about vortex diffusion and interaction has been obtained.

In this paper we present first the experimental aspects of our work. The velocity measurements, the lift measurements and the visualizations are given next. The comparison between the circulation computed from the tangential velocity profiles and from the lift measurements, as well as the interpretation of the interaction effects between a longitudinal vortex and a two dimensional airfoil follow. We conclude by pointing out the advantages of performing this type of investigation in a cavitation water tunnel instead of a wind tunnel.

II- EXPERIMENTAL

Tests were performed in the ENSTA Cavitation Tunnel fitted with a rectangular test section 80 mm wide and 150 mm high. In this work a three dimensional hydrofoil of elliptical planform, 40 mm maximum chord and 60 mm half span, was employed for generating the tip vortex. For the investigation of the interaction between the two foils, a 55 mm chord two

dimensional hydrofoil was incorporated into the test section 240 mm downstream of the vortex generating hydrofoil. Experiments were conducted at a free stream velocity of about 5 m/s and thus the Reynolds number of the three dimensional hydrofoil was about $2 \cdot 10^6$. Because of the relatively high turbulence level of the tunnel it is expected that laminar-to-turbulent boundary layer transition occurred on this foil.

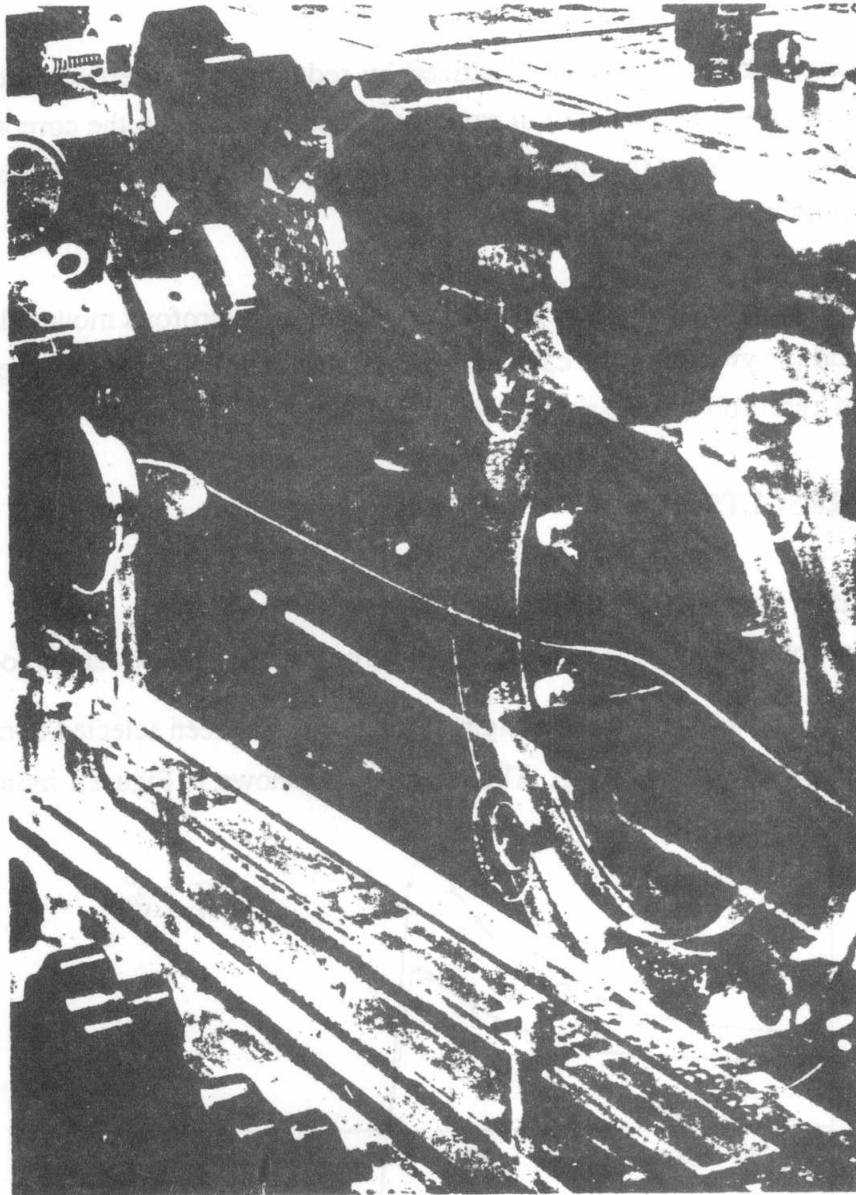


FIGURE 1: General view of the test section with the two hydrofoils mounted.
The path of the tip vortex core is indicated by the cavitation trace.

Mean velocities components on a transverse plane situated 200 mm downstream of the upstream hydrofoil were conducted in the absence of the two dimensional hydrofoil using a DISA LDA system operating in the back scattering mode. Problems associated with velocity measurements in a tip vortex were mainly due to the difficulty of accurately determining its

axis. In our case, the measuring volume, defined by the crossing of the splitted laser beam, was lead to illuminate the bubbles convected within the core at incipient cavitation conditions. From this position a new one was searched by determining the maximum of the vertical velocity component at a small distance, $\sim 1\text{mm}$, of the supposed vortex axis. However precise this positionning may be, it should be understood that a slight deviation from the true axis may cause, as it will be seen later, a dissymetry of the tangential velocity profiles.

The path of the tip vortex core was visualized by reducing the reference pressure in the downstream reservoir of the tunnel until cavitation conditions within the core were reached. The flow modifications near the surface of the downstream hydrofoil were also visualized through the cavitation occurrence.

Figure 1 shows a general view of the test section with both hydrofoils mounted. The path of the tip vortex and the growth of the cavitating core in the vicinity of the low pressure side of the downstream hydrofoil are clearly visible on this photograph.

III- RESULTS

III.1- Tangential Velocities

Figure 2 shows typical tangential velocity profiles for a single free stream velocity and two incidence angles, α , of the foil. The origin of the y axis has been selected to coincide with the tunnel wall closest to the wing tip. The visualization shown in Figure 1 indicates that the

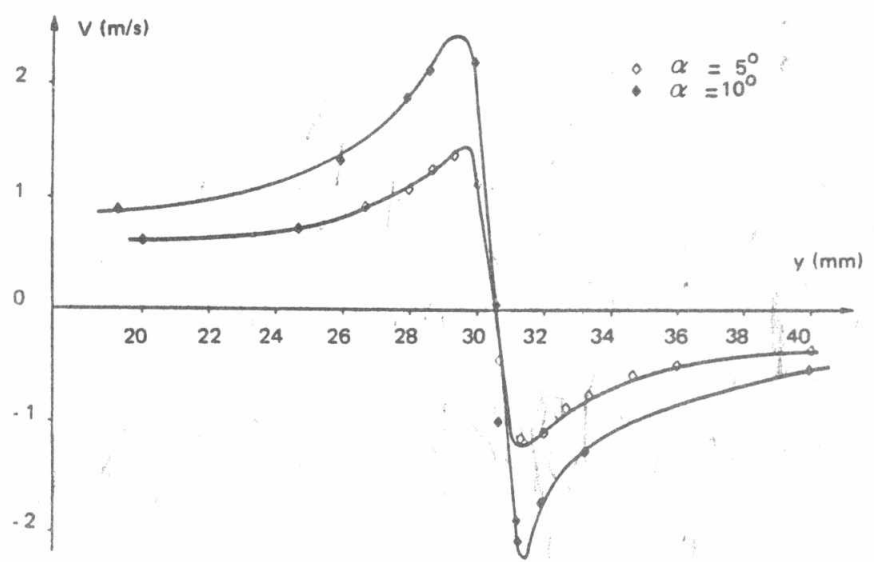


FIGURE 2: Tangential velocity components as a function of distance for two incidence angles.

vortex roll-up has been completed at the measuring station situated a few centimeters ahead of the downstream hydrofoil. Several interesting features of the velocity profiles are worthy of consideration: i) the axis of the vortex is situated at about 10 mm of the tip towards the mid section, ii) The rigid body rotation and the near potential regions are well defined, and iii) a slight dissymmetry due to the wing wake and to wall effects occurs. The size of the core is of about a millimeter and the slope of the velocity profile is extremely pronounced in the inner region. Very slight variations of the position of the vortex axis may thus lead to significant modifications of the velocities measured there.

The tangential velocity profile can be described by the Rankine vortex model,

$$V = \Gamma r / 2\pi a^2 \quad \text{for } r \leq a \quad (1)$$

and,

$$V = \Gamma / 2\pi r \quad \text{for } a \leq r \quad (1')$$

Such a model does not describe the transition region and a more appropriate description is given by the Burgers model,

$$V = \Gamma [1 - \exp(-Br^2)] / 2\pi r \quad (2)$$

where $B = (1.12/a')^2$ and a' is the radius where the maximum tangential velocity occurs.

Only the two lateral walls contribute to the wall effects since the upper and lower wall effects cancel one another by symmetry on the y axis. In Figure 3, the required row of vortices, limited to only two images, has been represented.

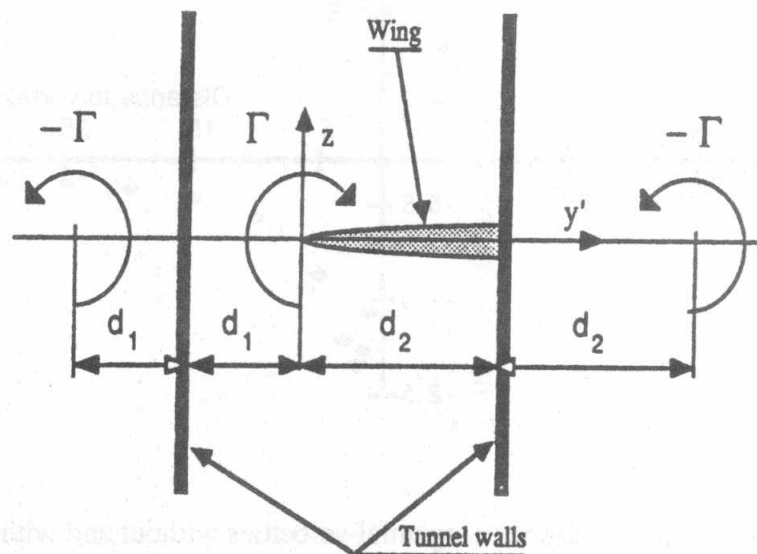


FIGURE 3: Vortex images required to account for the effect of the vertical walls

If the vortex strength is $\Gamma/2\pi$, the velocity at the position y' , measured from the main vortex axis, is given by,

$$V = -\frac{\Gamma}{2\pi y'} \frac{1 + \frac{y'^2}{4d_1d_2}}{\left(1 + \frac{y'}{2d_1}\right)\left(1 - \frac{y'}{2d_2}\right)} \quad (3)$$

Equations (2) and (3) can be combined to account for the wall effects on the velocity distribution given by the Burgers model on the horizontal axis y' ,

$$V = -\frac{\Gamma}{2\pi y'} \frac{1 + \frac{y'^2}{4d_1d_2}}{\left(1 + \frac{y'}{2d_1}\right)\left(1 - \frac{y'}{2d_2}\right)} (1 - e^{-By^2})$$

Figure 4 shows the tangential velocities for a vortex of strength $\Gamma = 0.0381 \text{ m}^2/\text{s}$ and $a' = 2.0 \text{ mm}$ depending on whether the wall effect is taken into account or ignored. The wall effect introduces a significant dissymmetry of the tangential velocity profile which partially justifies the one observed experimentally.

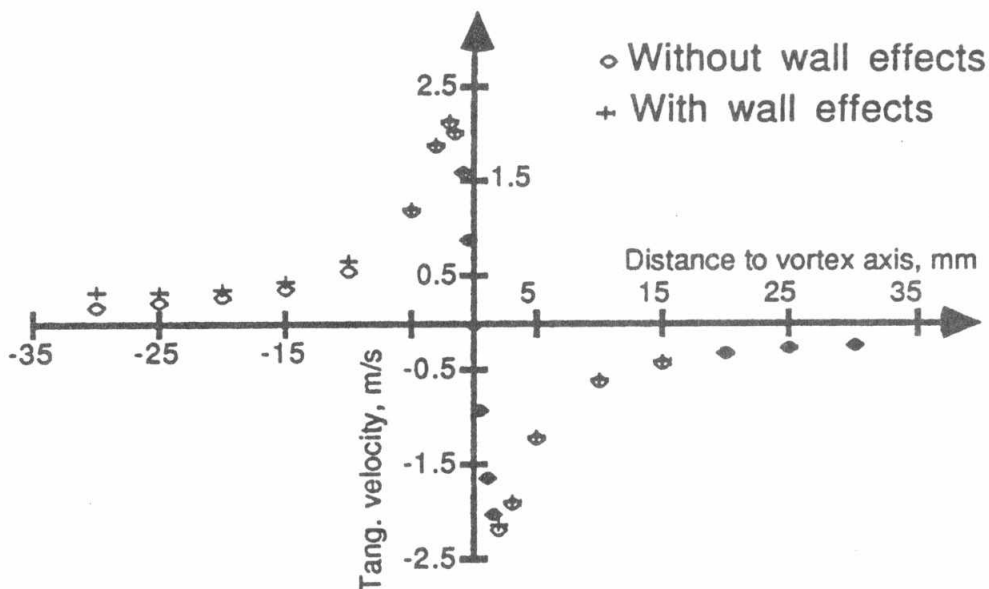


FIGURE 4: Computed discrete tangential velocities without and with wall effects

The value of Γ can be computed from expression (3) by fitting the velocities measured outside of the solid body and transition regions using a least square linear regression of $Y = \Gamma X$ where,

$$Y = V [2\pi y' (1 - y'/2 d_1) (1 + y'/2 d_2)]$$

and,

$$X = 1 + y'^2 / 4 d_1 d_2$$

The results of the computation for different flow conditions will be discussed in section IV.

III.2.-Axial Velocities

The axial velocities were measured in two orthogonal directions, y and z , and the results for an incidence angle of 10° are presented in Figure 5. A local reduction of the axial velocities is observed at the position corresponding to the vortex core. This wake-like behaviour has already been documented in [1] for much lower Reynolds numbers.

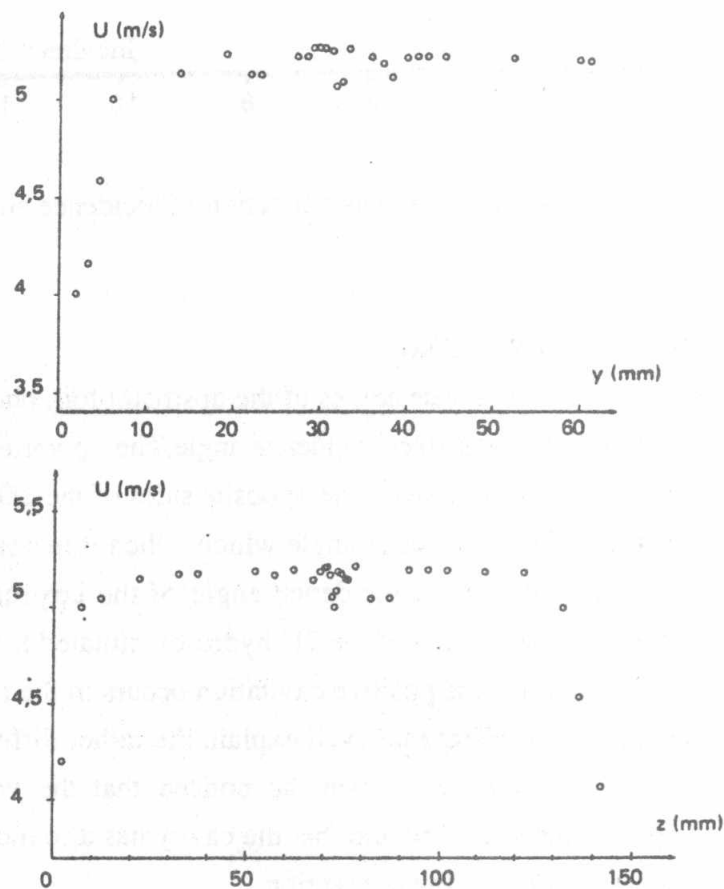


FIGURE 5: Axial velocity components measured in two orthogonal directions

III.3.-Force measurements

Both, lift and drag forces were measured using a two components strain gauge balance. Figure 6 shows that the lift coefficient increases linearly with the incidence angle up to about 7°. For larger values of the incidence angle the increase of the lift coefficient drops as a result of boundary layer separation.

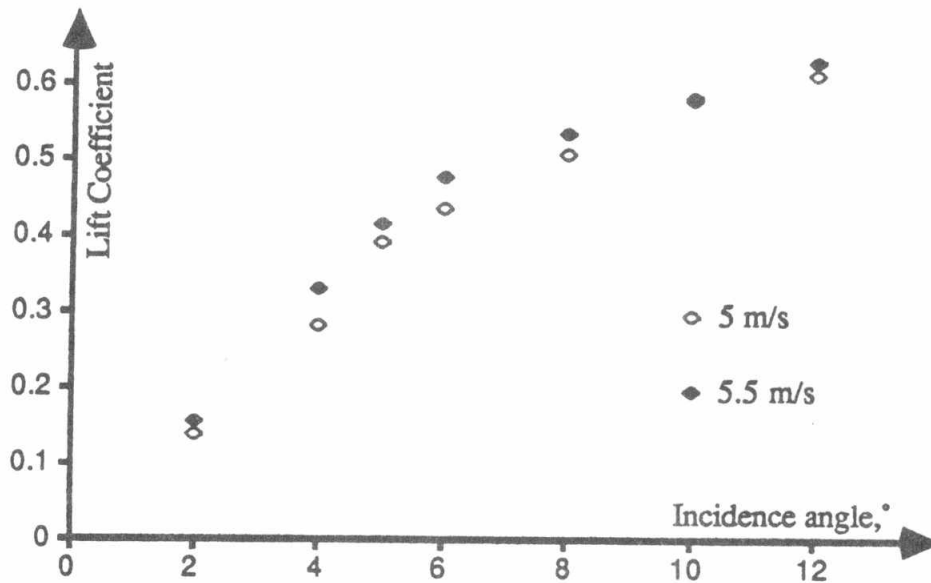


FIGURE 6: Lift coefficient as a function of incidence angle

III.4.-Visualization of vortex-wing interaction

Figure 7 shows, for two symmetric incidence angles of the upstream foil, photographs of the cavitation pattern on the 2D hydrofoil at a fixed incidence angle. The tip vortex rotates thus in opposite directions and cavitation occurs also on the opposite sides of the 2D hydrofoil. This is due to the local modification of the incidence angle which, when it increases, leads to an earlier local cavitation condition. When the incidence angle of the upstream hydrofoil is negative, cavitation is present on the portion of the 2D hydrofoil situated in the wake of the 3D hydrofoil. When the incidence angle is positive cavitation occurs in the region free from the influence of the wake. The wake effect may well explain the rather different superficial aspect of the cavitation pattern. Moreover, it can be noticed that the vortex line bends considerably when passing over the hydrofoil and that the cavity has a rounded lateral edge. These findings will be discussed in the following section.

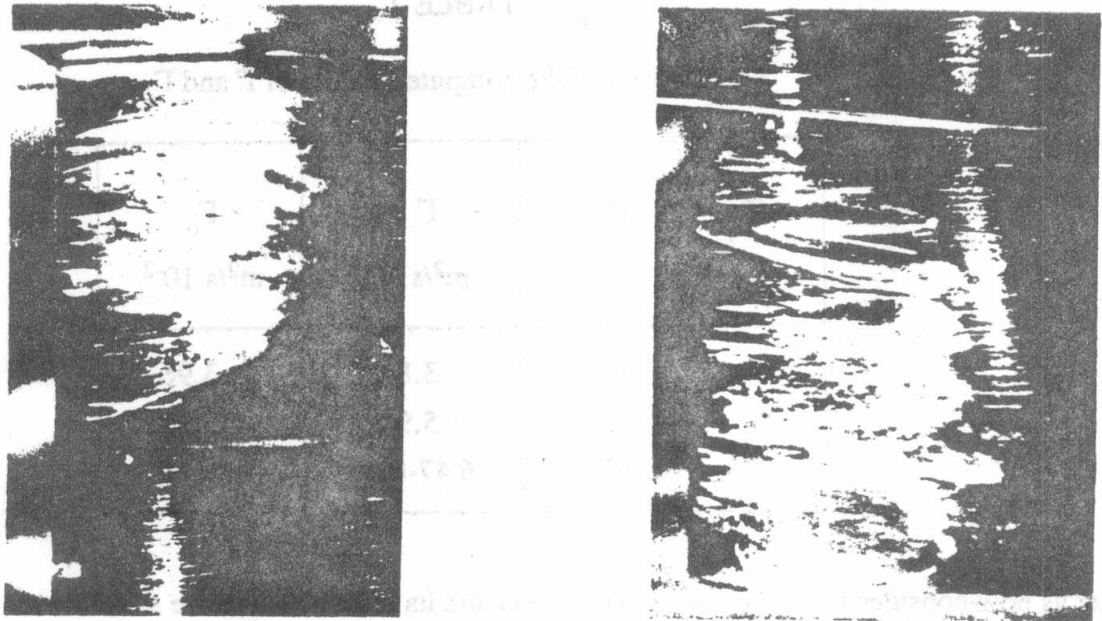


FIGURE 7: Cavitation pattern on a two dimensional hydrofoil downstream of a tip vortex
generating hydrofoil

- a) positive incidence angle of the upstream hydrofil
a) negative incidence angle of the upstream hydrofil

IV.-- DISCUSSION

The value of the circulation Γ of the tip vortex is generally assumed to be the maximum circulation Γ_0 over the hydrofoil. For an elliptical wing Γ_0 is given by [6],

$$\Gamma_0 = \frac{2LV_\infty C_L}{\pi\Lambda}$$

where L is the span of the wing, V_∞ the free stream velocity, C_L the lift coefficient, $\Lambda = L^2/S = 4L/\pi c_m$ is the aspect ratio, S the surface of the foil and c_m the maximum chord.

The values of Γ , computed as explained in III.1, and of Γ_0 are presented in Table I. For the

three cases investigated the agreement is satisfactory considering the accuracy of the velocity and lift measurements.

TABLE I

Comparison of the computed values of Γ and Γ_o

V_∞ m/s	α °	Γ m ² /s 10 ⁻²	Γ_o m ² /s 10 ⁻²
5	5	3.8	3.96
5	10	5.9	5.91
5.5	10	6.47-6.56	6.46

Let us now consider the vortex-wing interaction and its effects. These are as follows:

- a) upstream of the 2D hydrofoil the vortex line follows a streamline and induces, together with the vortex images required to account for the wall effects, a velocity field, with components on the transverse plane, superimposed on the axial flow. Thus, the 2D hydrofoil "sees" an upstream non uniform velocity field which determines a modification of the effective incidence of the foil along the width of the test section. When the local effective incidence angle increases, the pressure distribution is modified and, in particular, pressures on the upper surface of the foil are diminished. Therefore cavitation can occur earlier.
- b) over the 2D hydrofoil the vortex line bends because of the velocities induced by the vortex image required to satisfy the zero normal velocity condition on the surface of the hydrofoil, and,
- c) on the hydrofoil surface the transverse tangential velocity components induce a local yaw angle which explains the round lateral edge of the cavity.

V.- CONCLUSIONS

A small cavitation tunnel has proved to be a powerful tool in the investigation of tip vortex and tip vortex-wing interaction. Indeed, the path of the vortex can be easily visualized by reaching the conditions leading to the formation of a cavitating vapour core. Moreover, the

cavitation pattern on a 2D hydrofoil, downstream of the tip vortex generating hydrofoil, gives qualitative information on the flow modifications due to the rotating flow induced by the tip vortex.

AKNOWELEDGEMENTS

This work was supported by the Direction de Recherches, Etudes et Techniques (DRET), Ministry of Defense, FRANCE, under contract N° 83/1158. The experiments were conducted by S. AFLALO and D. BISMUTH to whom the author express his deep appreciation.

REFERENCES

1. Baker, G.R., Barker, S.J., Bofah, K.K. and Saffman, P. G., *Laser anemometry measurements of trailing vortices in water*, J. Fluid Mech., 65, 2, p. 325-336, 1974.
2. Souders, W.G. and Platzler, G.P., *Tip vortex cavitation and delay of inception on a three-dimensional hydrofoil*, David Taylor NSRDC Report 79/051, 1979.
3. Aflalo, S.S., Bismuth, D. and Fruman, D.H., *Tip vortex cavitation inhibition by polymer solution injection*, Rapport de Recherche ENSTA N°208, 1986.
4. McAlister, K.W. and Tung, C., *Interaction between an airfoil and a streamwise vortex*, AIAA 17th Fluid Dynamics, Plasma Dynamics and Lasers Conference, Snowmass, Colorado, USA, June 1984.
5. Higuchi, H., Rogers, M.F. and Arndt, R.E.A., *Characteristics of tip vortex noise*, Symposium on Cavitation and Multiphase Flow Noise, ASME Winter Annual Meeting, Anaheim, California, USA, December 1986.